Progress In Electromagnetics Research B, Vol. 30, 255–277, 2011

A LOW-COST PHASED ARRAY ANTENNA INTEGRATED WITH PHASE SHIFTERS COFABRICATED ON THE LAMINATE

P. Goel* **and K. J. Vinoy**

Department of Electrical Communication Engineering, Indian Institute of Science, Bangalore 560012, India

Abstract—This paper presents the design, development and experimental characterization of a monolithic phased array antenna integrated on a microwave laminate. A four-element linear antenna array is realized by cofabricating the corporate feed network, microstrip-CPW transitions, DC blocks, and mesoscale phase shifters on the same substrate. The phase shifters used here are electrostatically actuated and their operation is similar to that of the distributed MEMS transmission line phase shifters. Various components of the array are designed and are individually evaluated before fabricating together. The measured radiation pattern characteristics for this array shows a scan angle of 10° in the X-band. All fabrication processes employed here can be performed at a good printed circuit manufacturing facility. This simple approach of cofabricating various components can be readily extended for large phased arrays required in radar and space communication applications.

1. INTRODUCTION

With the increased use of radio frequency (RF) terminals capable of directing the radiated beam adaptively, possibilities for beam steering have gained much attention in communication and radar applications [1–6]. In radar systems, this feature is required to determine the direction of targets [7]. Modern radar systems require adaptive control of beam direction, beam shape, beam width, sidelobe level and directivity to improve the coverage and tracking resolution [5–7]. The amplitude and phase of radiated signal at each antenna

Received 11 April 2011, Accepted 10 May 2011, Scheduled 16 May 2011

* Corresponding author: Poonam Goel (poonam.goel13@gmail.com).

element is controlled to adjust side-lobe levels, conveniently locate nulls, and to shape the main-beam of radiation. These antenna systems differ in how the radiated beam is formed and steered. In large antenna systems, beam steering can be achieved mechanically or electronically. In mechanically steered antennas, beam scan is obtained by mechanically rotating a large gain antenna or an array. However mechanical scanning requires a physical positioning system that can be costly, especially when precision is required. In addition, mechanical scanning is often too slow for many applications [3]. On the other hand, in electronically steered antennas, the direction of the radiated beam is changed without any mechanical motion of the antenna system. Therefore, electronically steerable antennas offer advantages such as faster scan rate and the capability to track multiple targets, compared to mechanically scanned systems [1, 7].

Similarly, in terrestrial and space communication systems, both switched and steered beam approaches are used to improve the signal-to-noise ratio (SNR) and channel capacity [1–3]. In switched beam system, switching components are used in the RF front-end to switch the direction of radiated beam or the null to reduce cochannel interference. Such digital beam steering approaches [8] are practical and hence are currently popular up to low microwave bands. On the other hand analog radio frequency (RF) beam steering systems are required at higher frequencies. A phased array system, involving electronically controlled phase shifters offer beam steering capability [9]. Commercial phased array antenna systems for microwave applications are implemented by realizing most components on laminates. Active components such as amplifiers are realized on the conventional semiconductor substrates such as silicon, gallium arsenide (GaAs) utilizing semiconductor technology, packaged and attached to feed network to realize phase control modules in large phased arrays. Phase shifters, which are essential components in these systems, are also included in a similar fashion. This approach, not only makes such arrays expensive but also limit their performance as integration of packaged components invariably worsen the insertion loss, require matching networks and hence increase the overall size.

Monolithic microwave integrated circuits (MMIC) phase shifters, presently used in most phased arrays, are lossy and non-linear. In recent years, radio frequency micro-electromechanical systems (RF MEMS) technology has offered new possibilities for passive phase shifters on various substrate materials to overcome these disadvantages [10, 11]. If these could be integrated with the remaining components of the phase control module of phased arrays, better performing antenna systems at lower cost may result. Small monolithic

phased array antenna system for operating frequency 15 GHz is reported by Topalli et al. [11] on a glass substrate using distributed MEMS transmission line (DMTL) phase shifters with an overall size of $2.9\lambda \times 2.4\lambda$. Similarly, Ji et al. [12] reported phase shifters on silicon wafer using barium strontium titanate (BST) phase shifters for 15GHz which does not have any moving components. However, these monolithic phased array systems cannot be extended due to limited wafer size [13, 14]. In addition, the phase shifter in [11] is fabricated using surface micromachining process which suffers from challenges of reliability. Phase shifters with BST [12] usually require a very high DC bias voltage of 300 V.

In this paper, a monolithic phased array is demonstrated on a conventional microwave laminate substrate which can be easily extended for larger arrays as microwave laminates are available as large boards. Similar monolithic phased array previously reported on these laminates used complex printed circuit board processes which uses laser cutting, computer numerical controlled (CNC) milling, and thermo-compression bonding [15]. In contrast, the proposed phase shifter fabrication is simple, economical and can be cofabricated on laminates along with other components with marginally extended fabrication processes. In order to avoid the high cost of thin film deposition and processing in vacuum and/or clean room this uses add-on copper foils to realize moving structures. Realization of such Mesoscale Electrostatically actuated Phase shifter on microwave Laminate (MEPL) with operating principles similar to the micromachined DMTL phase shifter, is already demonstrated as isolated units [16].

This paper describes the design of various components of a four-element phased array to demonstrate the possibility of integration with this approach. Since these phase shifters are implemented on a coplanar waveguide, whereas feed networks and patch radiators are convenient on microstrip line technology, two microstrip-to-CPW transitions are required per phase shifter. Furthermore, the integration of these phase shifters into the system required additional DC bias and DC block features as indicated in Figure 1. The design aspects of these components are discussed in the next section. Detailed process steps for the fabrication of the phase shifter and the phased array are presented in Section 3. Experimental results for the phased array are presented in Section 4. These indicate that, this approach is suitable for a simple fabrication of a low-cost phased array antenna system that may be extended for larger arrays.

2. DESIGN OF COMPONENTS OF THE PHASED ARRAY ANTENNA

A schematic diagram with various components of a phased array antenna system is shown in Figure 1. The development of this system involves several electromagnetic design challenges. The design of the power distribution network is crucial in a phased array antenna to excite the array elements with the required amplitude and phase [17]. As this involves several branching networks, a power distribution network can be implemented easily using microstrip or stripline transmission lines in a corporate feed arrangement. However since the operation of the phase shifter requires variable shunt capacitors between the signal and ground, this is fabricated utilizing a CPW transmission line. Hence microstrip-CPW transitions are required on both ends of the phase shifter.

In addition, DC bias voltage is required for actuating these electrostatic beams. This requires addition of DC block and RF feed through in the circuit. These are integrated with the microstrip-CPW transitions to save space, without compromising the performance. The transition on the input side includes the DC-block to prevent the bias voltage at a phase shifter from reaching the RF source and the other

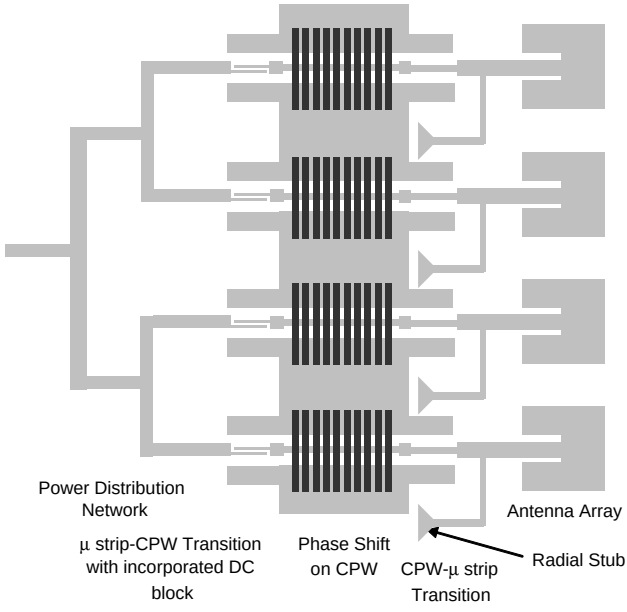

Figure 1. Schematic of the phased array system.

phase shifters. Radial stub is included at the other end of the phase shifter to avoid leakage of RF energy through the DC bias terminals.

The most important component of this array is the Mesoscale Electrostatically actuated Phase shifter on microwave Laminate (MEPL) with operating principles similar to the micromachined DMTL phase shifter [16]. Its fabrication approach does not use metal deposition/patterning process, thereby eliminating the need for high cost cleanroom and sophisticated equipment for film deposition. Instead copper foil (thickness = 15 µm) assembled above the CPW are used as moving bridge structures. Since these structural members are not from deposited thin films, stiction is not expected. Since this approach uses thicker metal layers, the power handling capability is expected to be significantly higher than micromachined phase shifters. Even though the present demonstration requires a high actuation voltage, the DC block feed through are designed to work in this range. This voltage requirement can possibly be reduced significantly by modifying the beam geometry using advanced lithographic approaches. All of the following components of the array are fabricated on an Arlon AD350 laminate (thickness = 30 mils, relative permittivity $\varepsilon_r = 3.3$ and loss tangent = 0.003):

1. Antenna element and array.
2. Power distribution network.
3. Microstrip-CPW transition with a radial Stub.
4. Microstrip to CPW transition with a DC-block.
5. Mesoscale electrostatically actuated phase shifter.

Details of their design and implementation are discussed in the following paragraphs.

2.1. Antenna Element and Array

Microstrip patch antenna has become one of the most convenient planar antenna element for small arrays. As these are fabricated by lithography techniques used in printed circuit board, manufacturing the overall cost of the antenna is minimum. The dimensions of the patch can be determined using standard formulae [17, 18]. In addition, this also offers the possibility of various feed approaches which could be selected based on the specific requirement. In this demonstration an inset fed microstrip patch antenna is used as the radiating elements for the linear array system because of its completely planar fabrication process.

2.1.1. Design of the Antenna Element

Analytically modelled length, width and inset feed point position of the patch are 9.3 mm, 10.8 mm and 3.3 mm respectively for design frequency 9.5 GHz. The analytical model is simulated in a finite element method-based 3D fullwave electromagnetic simulation program and is further optimized. The optimized length, width and inset feed point position (of patch antenna are 8.4 and 10.7 mm and 2.9 mm respectively for 9.5 GHz. Single inset feed patch antenna is characterized for return loss. Figure 2 shows the good agreement between measured with simulated data.

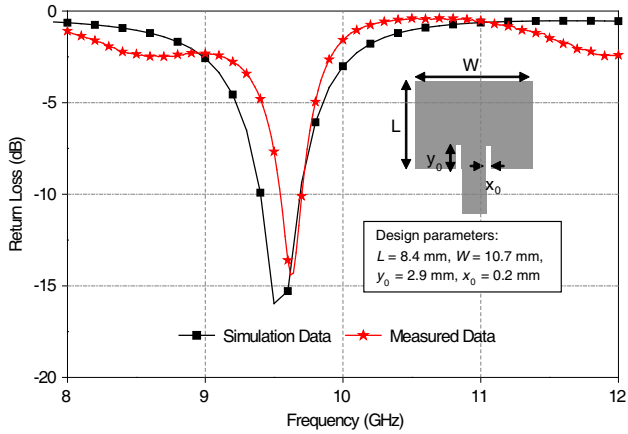

Figure 2. Comparison in simulated and measured return loss of a patch antenna.

2.1.2. Design of Linear Antenna Array

Spacing between antenna elements depends on the desired beam width and can be determined using [18].

$$\theta_m = 2\left[\frac{\pi}{2} - \cos^{-1}\left(\frac{\lambda}{Nd}\right)\right] \tag{1}$$

where, θ_m is the first null beamwidth, d is the separation between array elements and, λ is the free space wavelength. The beam direction is towards boresight and all elements are excited in phase.

In this demonstration, four identical elements consisting of the optimized microstrip patch antenna from the last sub-section is used in a linear array arrangement with uniform spacing. The array spacing is designed to have 10 dB beamwidth of 40°, so that the beam steering

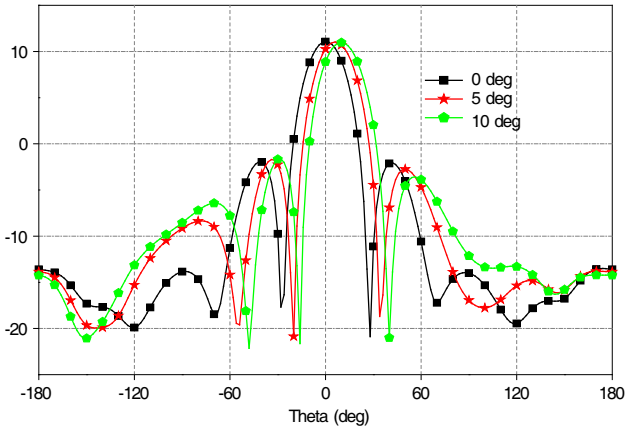

Figure 3. Demonstration of scanning of radiated beam in a four-element array. All elements have equal amplitude and are spaced at 17 mm. Cases with progressive phase shifts of 20° and 33° are compared with the reference uniform phase.

characteristics can be demonstrated with reasonable phase shift. The spacing between elements was found to be 17 mm. Figure 3 shows the simulated radiation characteristics which indicates a beam scan angle of 10° with progressive phase shift of 33° (excitation phases of elements at 0°–33°–66°–99°).

2.2. Power Distribution Network

A feed network consisting of two-stage two-way power dividers is used for feeding the four elements of the array. The design requirements include equal division of power between elements, good amplitude and phase balance, and impedance match. While the return loss at the feed port is considered, the isolation between output ports are not included in this demonstration. It is expected that the output impedance would be kept near 50 Ω so that reflections do not occur at these ports in the array environment. Since this is an integrated array, the locations of the output ports are required to agree with the locations of antenna elements in the array designed in the previous sub-section.

The design of each stage is similar to a Wilkinson power divider without the bypass resistor [19]. To ensure the impedance match at the input port, quarterwave transformers are included with output arms as shown in Figure 4. Three such power dividers are connected together to form the 4-way corporate feed arrangement. To keep the output ports (2 to 5) at the required locations with 17 mm between them,

additional transmission lines were required in all stages. In order to avoid coupling between parallel transmissions lines the spacing between the power divider at the first stage and those in stage II are separated by a gap g. It has been found that the phase and amplitude balance can be controlled by changing g. The corners of the transmission lines are tapered to reduce the insertion loss. Similarly a small notch is included at the vertices. All these adjustments were done using fullwave EM simulation software CST Microwave Studio. A gap of 7 mm was found to be sufficient in this regard.

The coupling between the input port and each of the output port is balanced well by extensive simulation modelling. Although ideally one would want these $S_{n1\,(n=2,3,4,5)}$ should be -6 dB for a 4-way power divider, the simulated S_{n1} was -6.6 dB at 9.5 GHz. The difference may be due to various losses in the microstrip line. Based on simulated parameters a 4-way corporate feed network is realized on Arlon AD350 utilizing standard PCB fabrication process. The photograph of the realized board is shown in Figure 5.

A comparison of the measured and simulation data for the fabricated four-way power divider network is described in Table 1.

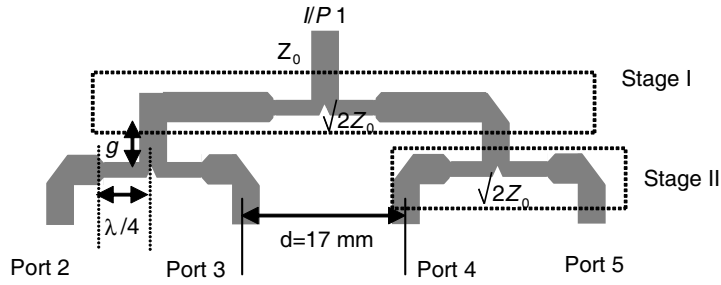

Figure 4. The geometry of a four-way corporate feed network configured using three power dividers.

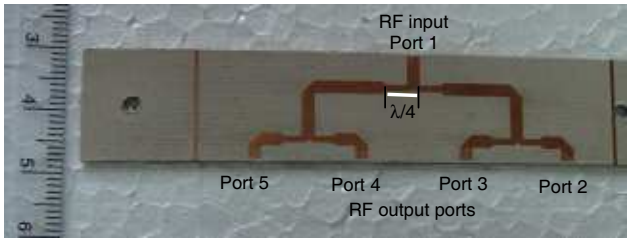

Figure 5. Photograph of a four-way corporate feed network realized.

Table 1. Comparison in measured data and simulation of feed network.

Specifications	Simulation data	Measured data
S_{11} (dB)	-24.4	-14.4
Max S_{n1} (dB) $n = 2, 3, 4, 5$	-6.6	-7.6
Amplitude Balance (dB)	± 0.13	± -0.7
Phase Balance (deg)	± 1.3	± 9

The measurements are performed by assembling the power divider with backside metallic. Difference in measured and simulation data may be due experimental errors caused in the assembly and soldering of SMA connectors. These results are acceptable for the present demonstration.

2.3. CPW-microstrip Transition and Bias Components

In this design of the phased array antenna, the phase shifter is realized on a coplanar waveguide (CPW) without ground on the backside. Since the antenna elements of the array consist of microstrip patches, and the corporate feed of microstrip line both with ground on the backside of the substrate, transitions are required. Several designs of microstrip to CPW transitions are reported in the literature [20–22]. It is also possible to design a transition when the signal traces of CPW and microstrip are continuous on one side of the substrate whereas electromagnetic coupling is used between the overlapped ground traces of CPW and microstrip which are on either side of this substrate [22]. To improve the performance further, shorting pins through vias which make physical contact between CPW with microstrip grounds are used in the present design. The transition consists of short sections of CPW and microstrip line, both of characteristic impedance Z_0 so that ports can be connected at the ends of the transition section as shown in Figure 6. The CPW part of the transition consists of in-plane ground traces that are parallel to the signal conductor. On the microstrip side, the ground trace is at the backside of the dielectric. The overlap between these ground traces can be optimized for the overall response of the transition.

The width of the microstrip transmission line for a characteristic impedance $50\,\Omega$ is found to be $1960\,\mu$m. On the CPW side, the signal trace is $1800\,\mu$m wide and is separated from the ground trace by $2200\,\mu$m. Initial length (L) and width (W) of transition are taken $4350\,\mu$m and $1020\,\mu$m respectively. Analytical modelled quarter

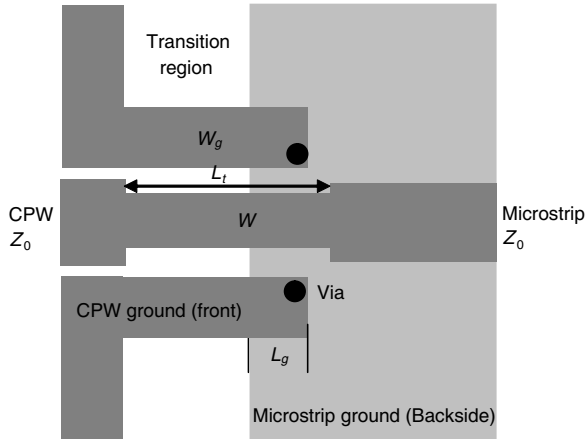

Figure 6. Schematic diagram of a CPW-microstrip transition.

wavelength is 4350 μm. Rigorous FEM simulations are performed in HFSS to optimize the final dimensions of the transition. Device with a total length of 5500 μm shows return loss of 26 dB but a high insertion loss of 0.968 dB at 9.5 GHz. Length, width and ground width (w_g) of transition section are optimized to improve the RF performance at the design frequency 9.5 GHz. Optimized design consists of transition section length of 5900 μm (L_t), signal conductor width (w) of 1400 μm, transition region ground (w_g) of 350 μm with ground overlap (L_g) of 3600 μm.

2.3.1. Microstrip-CPW Transition with DC Block Incorporated

In a phased array with corporate feed network, the bias applied to a phase shifter in one arm should not reach another arm. To provide this blocking, a DC block is connected between the phase shifter and the power divider. DC block is usually implemented with coupled transmission lines which are about quarter wavelength long for good insertion loss characteristics. Adding a DC block separately would therefore increase both the insertion loss and the physical dimensions. Since the transition as designed above is already quarter wavelength long, we tried to incorporate the DC block into this by replacing the continuous signal conductor in the transition section with a quarter wavelength long coupled line, while all other design parameter are kept same as in the transition.

In this design, the modified transition with DC block is implemented with a coupled line having fingers of width (w) 200 μm

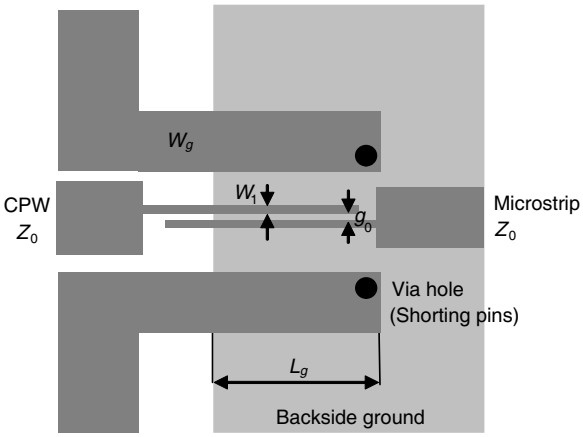

Figure 7. Schematic representation of microstrip-CPW transition with incorporated DC-block.

separated by gap (g_0) 200 µm while the pitch of CPW is kept 2200 µm throughout. In this geometry shown in Figure 7, shorting pins are used to make contact between the ground of microstrip and the ground traces of the CPW. The optimized width of transition ground (w_g) in this device is 290 µm and the overlap (L_g) between the ground conductors on either side of the dielectric is 1500 µm. The length of the coupled lines (3800 µm) is optimized for S-parameters at the design frequency of 9.5 GHz. Figure 8 shows a comparison of the S-parameters of this CPW-microstrip transition with the one without the DC block, as obtained from HFSS simulations. In both cases, the S_{11} is below −20 dB at the design frequency. These results also indicate that the insertion loss is marginally degraded to 0.776 dB at 9.5 GHz of transition without DC block. However, coupled line section with a gap (g_0) of 200 µm (limited by the fabrication) typically results in an insertion loss of 0.85 dB. As this additional loss is completely avoided, it may be concluded that by this approach of combining the two functions, one would get a significant improvement in the overall insertion loss.

2.3.2. CPW-microstrip Transition with a Radial Stub

A radial stub is required to connect the DC bias without affecting the RF performance of the signal. DC bias is used to electrostatically actuate the bridge structures of the phase shifter [10]. This DC Bias is applied across the signal conductor and ground of the CPW in the

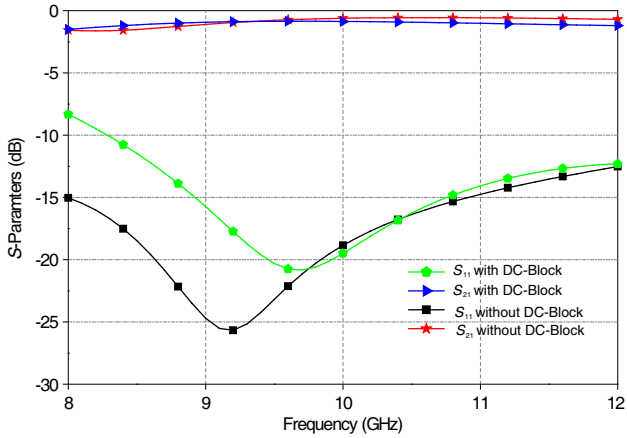

Figure 8. A comparison of the simulated S-parameters of the modified microstrip-CPW transition with a DC-block with the simple transition.

phase shifter. In the present design a radial stub is combined with CPW to microstrip transition at the antenna end of the phase shifter to minimize the overall footprint. Therefore the stub is connected to the signal conductor with a high impedance (130 Ω) interconnecting transmission line. This is limited by the minimum possible line width in the fabrication approach (line width = 200 μm). Keeping all the design parameters of CPW-microstrip transition as in Figure 6, this radial stub is connected to the microstrip line. The connecting conductor trace (L_r = 8000 μm) is bent toward CPW-microstrip transition as shown in Figure 9, to minimize the interference on the radiation pattern of the antenna. S-parameters of the transition with and without radial stub are shown in Figure 10, which indicates that radial stub is not seriously affecting the RF performance of the signal line at the frequency of interest.

As in the previous case of integrating the DC block with the CPW-microstrip transition, the addition of the radial stub has not degraded the overall performance. A comparison of the three transitions designed is summarized in Table 2.

2.4. Design of the Phase Shifter

A phase shifter is required on each arm of the phased array. The operation of this mesoscale electrostatically actuated phase shifter on microwave laminate (MEPL) is similar to that of a micromachined distributed MEMS transmission line (DMTL) phase shifter which

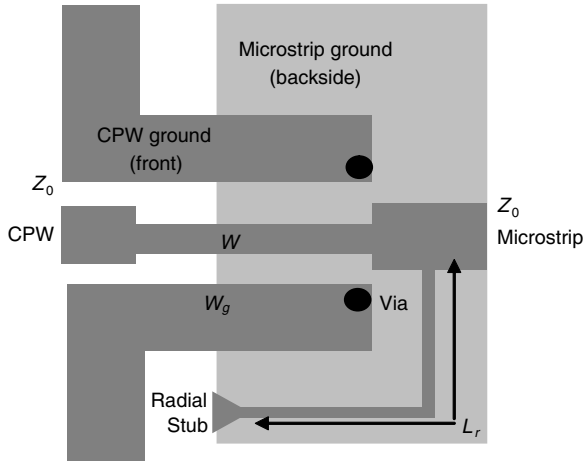

Figure 9. CPW-microstrip transition combined with the radial stub.

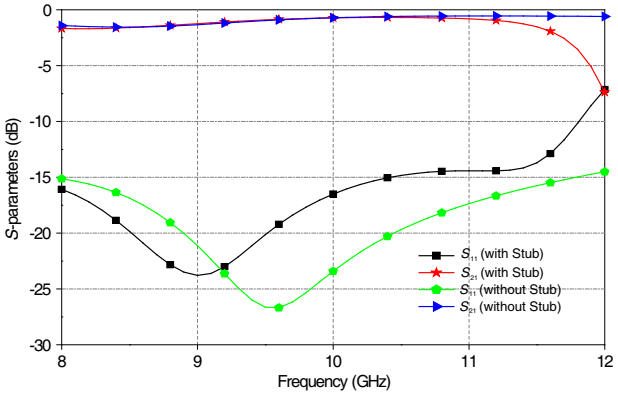

Figure 10. S-parameters of the transition with and without radial stub in HFSS simulation.

can be explained based on the changes in the phase velocity of a transmission line periodically loaded with shunt capacitors. These phase shifters have bridge structures, whose height can be varied by applying a DC bias, above a coplanar waveguide [10]. The separation between these bridges is so small that the capacitance due to these can be assumed to distribute along the length of a unit cell of such line. This distributed variable capacitance acts in parallel with the capacitance per unit length of the distributed model of a transmission line. Therefore the change in capacitance affects the characteristic impedance and phase constant of the line.

Table 2. Comparison of the design parameters and simulated performance of various CPW-microstrip transitions designed.

Parameter	Simple Transition (Figure 6)	Transition with DC block (Figure 7)	Transitions with Radial stub (Figure 9)
Transition Length (mm)	5.9	3.8	5.9
Overall width (mm)	17	17	17
Total Length (mm)	11.5	9.6	11.5
Insertion loss at 9.5 GHz (dB)	0.77	0.85	0.90
Bandwidth (2:1 VSWR) (GHz)	8–12	8–12	8–11.7

To ensure impedance matching for the loaded transmission line, the characteristic impedance of the unloaded line is kept high, often above 80 Ω. The change in characteristic impedance due to variation of height of these bridges can be made minimum when the line is properly designed. Unlike a MEMS switch, these bridges are not required to touch the conductor beneath, but are ensured to move within the linear range of operation. This stable range is determined based on structural and electromechanical parameters of the bridge structure. Physical parameters of the phase shifter obtained based on electromechanical modelling using Coventorware and electromagnetic modelling using CST microwave studio are summarized in Table 3. Figure 11 shows the scattering parameters of the phase shifter as the bridge height is varied between the original position and the maximum stable position. S_{11} is below −10 dB in 8–12 GHz range and insertion loss is better than −1 dB in these cases. Figure 12 indicates the phase shift obtained by changing the beam height.

Based on design values in Table 3, these phase shifters are fabricated on the laminate of the phased array. The cross sectional view and a photograph of a stand-alone phase shifter is shown in Figure 13 for better appreciation of the challenges in its fabrication. In this approach, the beam and spacer are made of patterned copper foils which are assembled on a microwave laminate on which a CPW is patterned. A high DC voltage needs to be applied between the centre

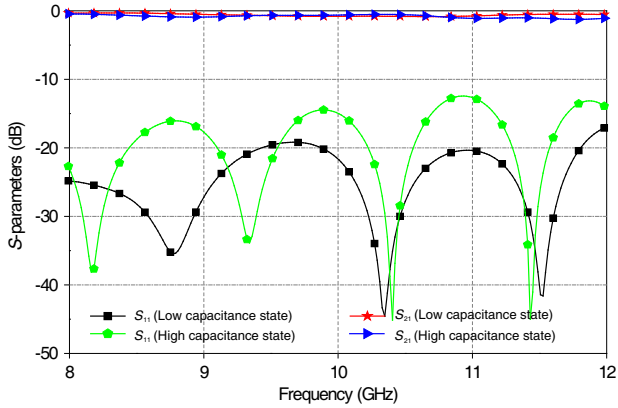

Figure 11. Simulated S-parameters of the phase shifter within its range of operation. The low capacitance state corresponds to the normal position of bridge structures, and the high capacitance is when the beams are actuated with the maximum possible voltage without causing pull-in. These simulations are obtained using fullwave electromagnetic simulation software CST microwave studio.

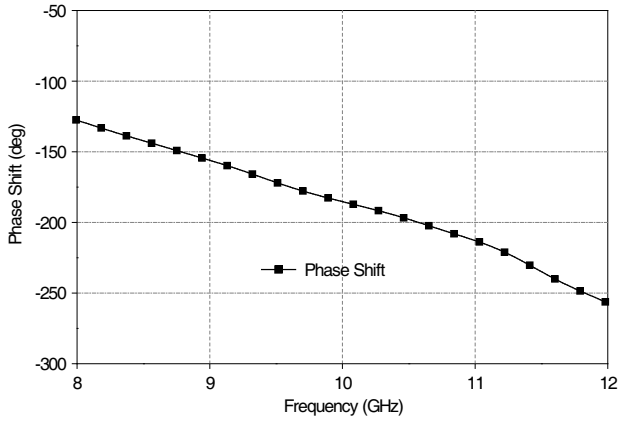

Figure 12. Phase shift calculated from phase of S_{21} obtained using CST simulations.

conductor of the CPW and the beam geometry to move these beams. The operation of the device requires that these structures are kept at a small height. The dielectric breakdown between the actuating electrodes is prevented by having an additional dielectric cover layer. These posed several challenges to be overcome for the reliable and repeatable integration of the phase shifter.

Table 3. Physical parameters of the phase shifter.

Design parameter	Value
Number of bridges	50
Beam length (μm)	4500
Beam length (μm)	200
Beam thickness (μm)	15
50 Ω CPW GSG configuration (μm)	200-1800-200
Width of bottom electrode (μm)	280
Spacer height (μm)	11
Dielectric(SU-8) thickness (μm)	4
Relative dielectric constant of SU-8-2002	4
Spacing between bridges (μm)	350
Young's modulus of beam material (GPa)	128
Maximum phase shift at 9.5 GHz (deg)	124
Voltage for maximum phase shift (V)	125.6

The laminate used for microwave components have surface roughness typically in the range of several micrometers. Based on optical profilometer measurements we have seen that the surface is uneven which is suspected to affect the dielectric breakdown characteristics of any protective thin film. Hence the patterned surface of the CPW is mechanically polished. Polishing is done in two steps, first with fine carbon particles powder which removes the microstructures but leaves the scratches on the surface. Scratches are reduced by polishing with diamond paste on nylon cloth. The signal conductor of the CPW is then covered with a dielectric (SU-8) to avoid the short circuit or arcing while actuating the beams, therefore increasing the device reliability. SU-8 is reported to have good dielectric strength. This is done by spin coating two layers of SU-2002. This is patterned to cover only the signal conductor area under the bridges.

Copper foils of 15 μ thickness are used as spacer as well as membrane. These are separately patterned to realize a window in the spacer and beam structures in the moving membrane by photo-chemical milling (PCM). Compared to the wet lithographic process, PCM can sure straightness of the patterned foils. A plexiglass sheet glued at the top of these layers to ensure they are kept snugly above the CPW, and to provide protection for the delicate beam structures. Wires are soldered to the radial stub and the ground electrode of CPW

to provide the DC bias required for the operation of the phase shifter. The measured phase shift of a phase shifter is shown in Figure 14. This response is not monotonous due to the impedance mismatches caused in the measurements as biasing wires are directly attached for these measurements as shown in the photograph of Figure 13(b). However the measured results on two fabricated prototypes agree well (Table 4).

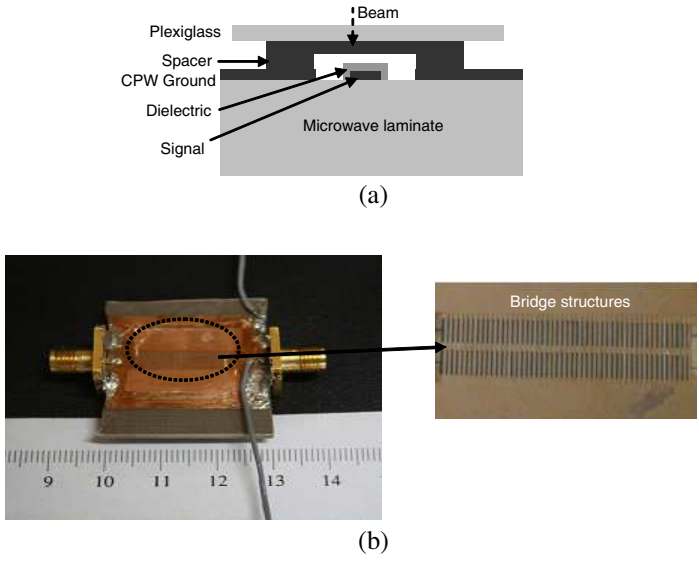

Figure 13. (a) Schematic of phase shifter on microwave laminates. (b) Photograph of a fabricated phase shifter (enlarged view of periodically distributed bridges).

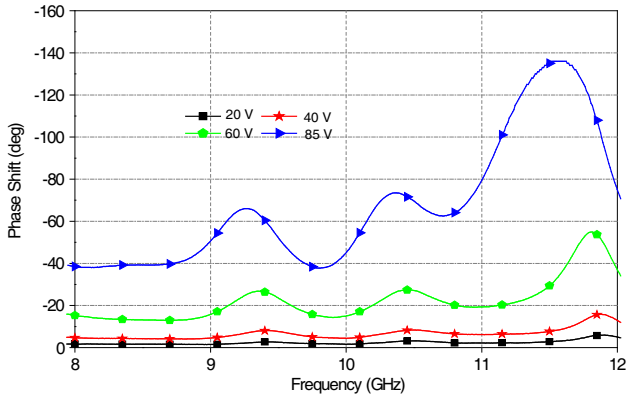

Figure 14. Measured phase shift of the phase shifter.

This approach for the fabrication of phase shifter is simple and economical and therefore can be extended for cofabrication of phase shifters on the microwave laminates along with other components of the phased array with marginally extending the PCB fabrication processes. The use of patterned copper foils eliminates the need for high cost of thin film deposition or their processing in vacuum and/or clean room environment. As these copper foils are thicker than deposited thin films and hence be expected to provide better power handling capability for these phase shifters. These structures are not prone to stiction which is a perennial problem in many microfabricated components. Although the voltage required is high, the device has sufficient built-in protection and isolation mechanisms and therefore can be extended for the use in phased arrays. The characterization of the completely integrated phased array on the laminated cofabricated with these phase shifters is discussed next.

3. INTEGRATION AND CHARACTERIZATION OF THE PHASED ARRAY

The photograph of the monolithic phased array antenna system on a microwave laminate using a cofabricated phase shifter operating with electrostatic principles is shown in Figure 15. In this system, components such as DC block and bias tee are integrated into the CPW-microstrip transitions to optimize the space and performance. After separately testing most components of this phased array antenna, the integrated phased array antenna is fabricated and tested for its beam steering capability. The copper layer on the Arlon microwave laminate is patterned by a 'print and etch' process. This uses a dry film photo-resist which is first laminated on the PCB metallization layer and patterned using wet chemical etching using ferric chloride. The additional copper foil layers and plexiglass cover are attached to the region with the phase shifter. Since this device consists of microstrip transmission lines and patch elements on either side of the phase shifter block, microstrip ground metal patches are patterned are on the backside of the substrate. The ground traces of CPW on the

Table 4. Comparison in RF performance of two identically fabricated devices.

@ 10 GHz	Device 1	Device 2
Phase shift (deg)	−60	−63
Reflection loss (dB)	−20	−20

front side are connected to these by shorting vias. Wires are soldered to the radial stubs and to a common ground conductor to apply the DC bias voltage to actuate the phase shifters.

In this demonstration an Aplab DC power supply of 0–300 V is used to provide the DC bias to the phase shifters. DC Voltages to individual phase shifters are provided by a simple resistive voltage divider network. The outputs of this divider are approximately at 0–0.5 V–0.7 V–V, where V is the DC supply voltage. It may be noted that the beam deflection and hence capacitance change due to

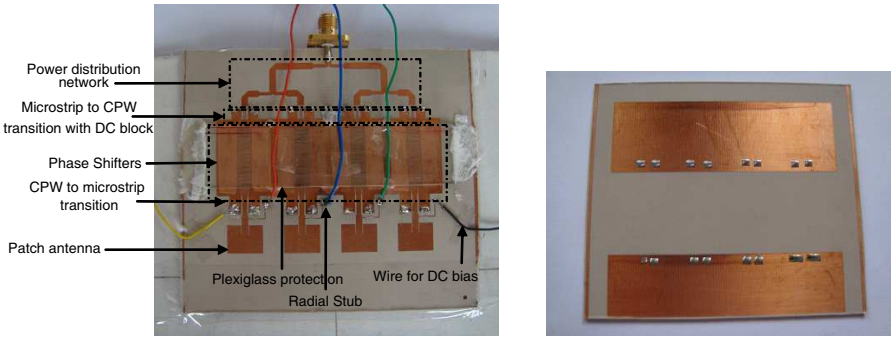

Figure 15. (a) Photograph of the integrated phased array antenna cofabricated phase shifter. (b) The backside view shows ground metal for microstrip power distribution network and antennas.

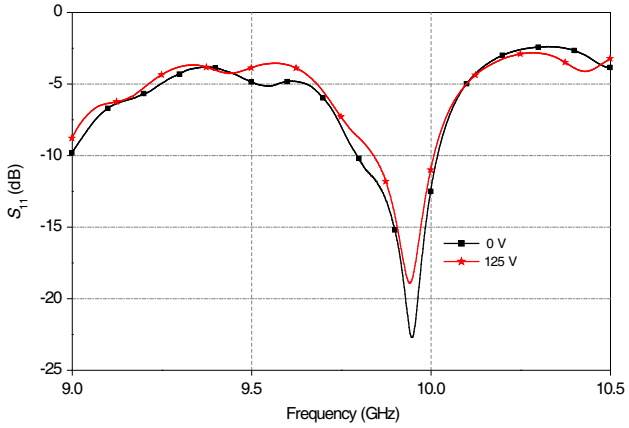

Figure 16. Measured S_{11} of the phased array with DC bias applied to the voltage divider network controlling phase shifters.

actuation are not linearly proportional to the voltage applied. Hence this combination of voltages is expected to a progressive phase shift of about 33°. Figure 16 presents the S_{11} response of the phased array antenna integrated with all components, without any bias voltage and with 125 V bias applied to the voltage divider network for the phase shifters. These indicate that the operating frequency has shifted to 9.8 GHz. This may be due to minor changes in the input impedances of various components integrated together. Since the smallest critical dimension of this device is 15 μm and the overall dimensions stretch to 7.1 cm ×7.6 cm, the complete device could not be simulated in any of the electromagnetic simulation softwares. Hence the interaction between various components of the system could not be included in the simulations.

The beam steering measurement of the phased array is performed in an anechoic chamber. The radiation pattern is recorded at 9.8 GHz in the azimuth plane by applying 125 V to the voltage divider network. The minor squint in the original beam may be due to amplitude and/or phase imbalance between various arms. As noted before, this could not be evaluated accurately due to the large systems size. Furthermore, as various layers are assembled, there could be minor differences in the thickness from expected values. This may also have caused the pattern to show a higher than expected (−13.6 dB) sidelobe level. On

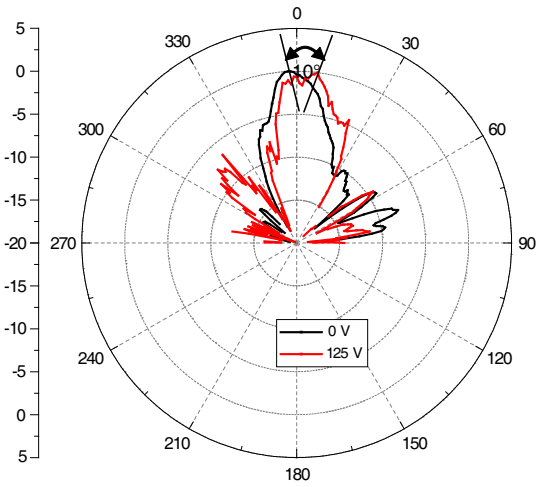

Figure 17. Results of beam steering measurements on the phased array system at 9.8 GHz, by applying 0 V and 125 V to the voltage divider network controlling the phase shifters.

the application of the bias, the beam shifts by 10° as shown in Figure 17 which meets the present specification. However, the beam scan angle can be increased by increasing the phase shift by modifying the phase shifter design to include larger number of bridges. As the beam shifts, there is also a minor change in the beam width. This indicates that the applied phases are not progressively varying. These may be rectified by designing suitable digitally controlled buck converter for controlling these phase shifters.

4. CONCLUSIONS

This paper demonstrates the possibility for monolithic integration of electrostatically actuated phase shifters with other components to realize a phased array antenna system on a commercial microwave laminate. This phase shifter is fabricated directly on the laminate by a recently developed procedure. Since the phase shifter is on a coplanar waveguide (CPW), and other components of the array such as power divider network and radiating elements are on microstrip configuration, CPW-microstrip transitions are also designed for this integrated system. To compactly provide DC blocking between various elements, coupled line sections are integrated with these transitions, without affecting their RF performance. When the required DC bias voltages are applied to various phase shifters, the realized array shows a beam scan of 10°.

Although electrostatically actuated RF MEMS phase shifters were developed about a decade back to improve on the insertion loss and non-linear characteristics of MMIC phase shifters, these microfabricated components suffer from low power handling capability and reliability issues due to stiction. Furthermore, packaging technology for these devices is not matured yet, leading to high cost in packaged components and affecting their widespread use in phased arrays. In contrast, the electrostatically actuated phase shifter demonstrated here overcomes most of these challenges while retaining their advantages over MMIC, and can be fabricated by a very simple and extremely low cost approach. Furthermore, since these phase shifters are fabricated directly on laminate boards typically used for microwave components, this approach could be easily extended for larger arrays in a similar fashion. This is in contrast to micromachined monolithic phased arrays which are limited by the number of elements that can be accommodated within the size of substrates. The fabrication approach proposed here requires only minor modifications to conventional PCB manufacturing processes widely used for implementing microwave components.

REFERENCES

1. Fenn, A. J., *Adaptive Antennas and Phased Arrays for Radar and Communications*, Artech House, Boston, 2007.
2. Ohmori, S., Y. Yamao, and N. Nakajima, "The future generations of mobile communications based on broad-band access technologies," *IEEE Commun. Mag.*, Vol. 38, 134–142, 2000.
3. Ehmouda, J., Z. Briqech, and A. Amer, "Steered microstrip phased array antennas," *World Academy of Science, Engineering and Technology*, Vol. 49, 319–323, 2009.
4. Godara, L. C., "Applications of antenna arrays to mobile communications. Part I: Performance improvement, feasibility, and system consideration," *Proc. IEEE*, Vol. 85, No. 7, 1031–1060, 1997.
5. Mailloux, R. J., *Phased Array Antenna Handbook*, 2nd edition, Artech House, Boston, 2005.
6. Hansen, R. C., *Phased Array Antennas*, John Wiley & Sons, Inc., New York, 2009.
7. Skolnik, M. I., *Radar Handbook*, 3rd edition, McGraw Hill, New York, 2008.
8. Schaer, B., K. Rambabu, J. Bornemann, and R. Vahldieck, "Design of reactive parasitic elements in electronic beam steering arrays," *IEEE Transactions on Antennas and Propagation*, Vol. 53, No. 6, 1998–2003, Jun. 2005.
9. Koul, S. K. and B. Bhat, *Semiconductor and Delay Line Phase Shifters*, Artech House, 1992.
10. Varadan, V. K., K. J. Vinoy, and K. A. Jose, *RF MEMS and Their Applications*, John Wiley & Sons, Inc., London, 2002.
11. Topalli, K., Ö. A. Civi, S. Demir, S. Koc, and T. Akin, "A monolithic phased array using 3-bit distributed RF MEMS phase shifters," *IEEE Transactions on Microwave Theory and Techniques*, Vol. 56, No. 2, 270–277, Feb. 2008.
12. Ji, T., H. Yoon, J. K. Abraham, and V. K. Varadan, "Ku-band antenna array feed distribution network with ferroelectric phase shifters on silicon," *IEEE Transactions on Microwave Theory and Techniques*, Vol. 54, No. 3, 1131–1138, Mar. 2006.
13. Kingsley, N., G. E. Ponchak, and J. Papapolymerou, "Reconfigurable RF MEMS phased array antenna integrated within a liquid crystal polymer (LCP) system-on-package," *IEEE Transactions on Antennas and Propagation*, Vol. 56, 108–118, Jan. 2008.
14. Gautier, W., V. Ziegler, A. Stehle, B. Schoenlinner, U. Prechtel,

and W. Menzel, "RF-MEMS phased array antenna on low-loss LTCC substrate for Ka-band data link," *EuMC 2009, IEEE European Microwave Conference*, 914–917, Sep. 29–Oct. 1, 2009.

15. Sundaram, A., M. Maddela, R. Ramadoss, and L. M. Feldner, "MEMS-based electronically steerable antenna array fabricated using PCB technology," *Journal of Micro-electromechanical Systems*, Vol. 17, No. 2, 356–362, Apr. 2008.
16. Goel, P. and K. J. Vinoy, "An electrostatically actuated phase shifter on printed circuit board for a low cost phased array antenna," *National Conference on MEMS, Smart Structures and Materials*, Central Glass and Ceramic Research Institute, Kolkata, India, Oct. 14–16, 2009.
17. Lo, Y. T. and S. W. Lee, *Antenna Handbook*, Vol. 3, Springer, 1993.
18. Balanis, C. A., *Antenna Theory Analysis and Design*, 2nd edition, John Wiley & Sons, Inc., New York, 1997.
19. Pozar, D. M., *Microwave Engineering*, 3rd edition, John Wiley & Sons, Inc., Singapore, Asia, 2005.
20. Simon, R. N., *Coplanar Waveguide Circuits, Components and Systems*, John Wiley & Sons, Inc., New York, 2001.
21. Strauss, G., P. Ehret, and W. Menzel, "On-wafer measurements of microstrip-based MMICs without via holes," *IEEE MTT-S International Symposium*, Vol. 3, 1399–1402, San Francisco, CA, USA, Jun. 17–21, 1996.
22. Robertson, R., E. M. Tentzeris, T. J. Ellis, and L. P. B. Katehi, "Characterization of a CPW-MS transition for antenna applications," *IEEE Antennas and Propagation Society International Symposium*, Vol. 3, 1380–1383, Atlanta, GA, USA, Jun. 21–26, 1998.